Theoretical Study of Two-Photon Absorption Properties of a Series of Double-Layer Paracyclophane Derivatives

Xin Zhou, Ai-Min Ren, Ji-Kang Feng,* and Xiao-Juan Liu

State Key Laboratory of Theoretical and Computational Chemistry, Institute of Theoretical Chemistry, Jilin University, Changchun 130023, China

Received: October 11, 2002; In Final Form: January 5, 2003

The equilibrium geometries, electronic structures, and one- and two-photon absorption properties of a series of paracyclophane derivatives have been determined by using the AM1 and ZINDO methods. The results show that the paracyclophane core as a multidimensional tunneling barrier remarkably increases the two-photon absorption cross section of molecules. As far as this series of paracyclophane derivatives is concerned, there exists a nonconventional "through-space" charge transfer. Our theoretical findings are consistent with recent experimental observations. It is found that the molecular length plays the most crucial role in the one-photon absorption intensity and the two-photon absorption cross section. For molecules with a given framework, a symmetrical structure with strong donor groups can result in a maximum two-photon absorption cross section. The three-state approximation is applicable to this series of paracyclophane derivatives. It is notable that paracyclophane-based molecules may afford advantages in the tradeoff of nonlinearity and transparency by generating a strong NLO response while providing a favorable displacement of the region of transparency.

1. Introduction

The two-photon absorption (TPA) process has been the subject of fast-growing interest in fields such as chemistry, photonics, and biological imaging because of a variety of applications of TPA dyes to upconverted lasing,[1−3] optical power limiting,[4−6] photodynamic therapy,[7] and 3D microfabrication.[8−10] The development of two-photon technology depends much on the success of synthesizing new molecules with large TPA cross sections at desirable wavelengths.[11−14] It is found that the molecular structure has a significant influence on the TPA cross section of molecules so that the study of the relationship between molecular structure and the TPA cross section is quite important. There exist various design strategies employed to enhance the magnitude of the TPA cross section of dyes.[11−20] Among them, increasing the dimensionality of charge-transfer networks is an especially important one. The TPA of a class of 2-D cumulene-containing polyenes was theoretically investigated by Norman, Luo, and Ågren.[15] They showed that the donor−acceptor substituted cumulenes containing aromatic molecules have large TPA cross sections, which are quantitatively comparable to those of the TPA dyes studied by Kogej et al.[16] Minhaeng Cho et al.[17] investigated the TPA properties of another series of octupolar molecules. They pointed out that for this kind of molecule the TPA cross section increases as the strength of the donor or acceptor increases; the TPA cross section is linearly proportional to the first hyperpolarizability. Lately, using a degenerate four-wave mixing technique, Sahraoui and co-workers measured the third-order susceptibilities and TPA in branched olgothienylenevinylenes derivatives. They demonstrated that the values of third-order susceptibilities and TPA coefficients β increase as the number of branches increases.[18] It is known that the increased conjugated length or scope of π-electron delocalization leads to a higher nonlinearity in the optical response, but at the same time, it results in a lower transparency in the spectral region of interest, limiting the potential usefulness of the material. So the conflict between them is worth being taken into account.

In this paper, we investigate the TPA properties of a series of paracyclophane derivatives with double-layer structure. The [2,2] paracyclophane bridge was chosen to serve as the locus of interchromophore contact since it enforces the cofacial overlap of two phenyl rings, minimizes intramolecular motion, and has proven useful for the study of $\pi-\pi$ electron delocalization and ring strain in organic compounds.[21,22] Furthermore, paracyclophane-based molecules may afford advantages in the tradeoff of nonlinearity and transparency by generating a strong NLO response while providing a favorable displacement of the region of transparency. Here, we will depict the optimized geometric structure of the paracyclophane segment and then discuss the impact of the conjugated length, donor (D) or acceptor (A) strength, and increased dimensionality on the TPA cross sections of molecules.

2. Theoretical Methods

The TPA process corresponds to the simultaneous absorption of two photons. The TPA efficiency of an organic molecule, at optical frequency $\omega/2\pi$, can be characterized by the TPA cross section $\delta(\omega)$. It can be directly related to the imaginary part of the second hyperpolarizability $\gamma(-\omega; \omega, \omega, -\omega)$ by[23]

$$\delta(\omega) = \frac{8\pi^2\hbar\omega^2}{n^2c^2}L^4\{\mathrm{Im}\}\gamma(-\omega; \omega, \omega, -\omega) \qquad (1)$$

where $\hbar$ is Planck's constant divided by 2π, n is the refractive index of the medium, c is the speed of light, and L is a local field factor (equal to 1 for vacuum).

* Corresponding author. E-mail: Jikangf@yahoo.com. Fax: +86-431-8945942.

10.1021/jp027184j CCC: $25.00
Published on Web 02/21/2003

The SOS expression used to evaluate the components of the second hyperpolarizability γ_{ijkl} can be derived by using perturbation theory and the density matrix method. By considering a power expansion of the energy with respect to the applied field, the γ_{ijkl} Cartesian components are given by[24,25]

$$\gamma_{ijkl}(-\omega_\sigma; \omega_1, \omega_2, \omega_3) = \frac{4\pi^3}{3h^3} \mathrm{P}(i, j, k, l; -\omega_\sigma; \omega_1, \omega_2, \omega_3)$$

$$\left[\sum_{m\neq o} \sum_{n\neq o} \sum_{p\neq o} \frac{\langle o|\mu_i|m\rangle\langle m|\bar{\mu}_j|n\rangle\langle n|\bar{\mu}_k|p\rangle\langle p|\mu_l|o\rangle}{(\omega_{mo} - \omega_\sigma - \mathrm{i}\Gamma_{mo})(\omega_{no} - \omega_2 - \omega_3 - \mathrm{i}\Gamma_{no})(\omega_{po} - \omega_3 - \mathrm{i}\Gamma_{po})} \right. \quad (2)$$

$$\left. - \sum_{m\neq o} \sum_{n\neq o} \frac{\langle o|\mu_i|m\rangle\langle m|\mu_j|o\rangle\langle o|\mu_k|n\rangle\langle n|\mu_l|o\rangle}{(\omega_{mo} - \omega_\sigma - \mathrm{i}\Gamma_{mo})(\omega_{no} - \omega_3 - \mathrm{i}\Gamma_{no})(\omega_{no} + \omega_2 - \mathrm{i}\Gamma_{no})} \right]$$

where $\mathrm{P}(i, j, k, l; -\omega_\sigma; \omega_1, \omega_2, \omega_3)$ is a permutation operator defined in such a way that for any permutation of (i, j, k, l) an equivalent permutation of $(-\omega_\sigma; \omega_1, \omega_2, \omega_3)$ is made simultaneously; $\omega_\sigma = \omega_1 + \omega_2 + \omega_3$ is the polarization response frequency; $\omega_1, \omega_2, \omega_3$ indicate the frequencies of the perturbing radiation fields (considering the degenerate TPA, $\omega_1 = \omega_2 = \omega$ and $\omega_3 = -\omega$); i, j, k, and l correspond to the molecular axes x, y, and z; m, n, and p denote excited states and o, the ground state; μ_j is the $j(= x, y, z)$th component of the dipole operator; $(\langle m|\bar{\mu}_j|n\rangle = \langle m|\mu_j|n\rangle - \langle o|\mu_j|o\rangle)$; $(h/2\pi)\omega_{mo}$ is the transition energy between the m and o states; and Γ_{mo} is the damping factor of excited state m. Considering the higher the excited state is the shorter its lifetime, Γ_{mo} is expressed as follows:[26]

$$\Gamma_{mo} = 0.08 \times \frac{\omega_{mo}}{\omega_{1o}} \quad (3)$$

To compare the calculated δ value with the experimental value measured in solution, the orientationally averaged (isotropic) value of γ is evaluated, which is defined as

$$\langle\gamma\rangle = \frac{1}{15} \sum_{i,j} (\gamma_{iijj} + \gamma_{ijij} + \gamma_{ijji}) \qquad i, j = x, y, z \quad (4)$$

Hereafter, $\langle\gamma\rangle$ is taken into eq 1, and then the TPA cross section $\delta(\omega)$ is obtained.

Generally, the position and relative strength of the two-photon resonance are to be predicted using the following simplified form of the SOS expression:[27]

$$\delta \propto \frac{M_{0k}{}^2(M_{kn}{}^2 + \Delta\mu_k{}^2)}{(E_{0k} - E_{0n}/2)^2\Gamma} \quad (5)$$

where M_{ij} is the transition dipole moment from state i to j; E_{ij} is the corresponding excitation energy; the subscripts 0, k, and n refer to the ground-state S_0, the intermediate state S_k, and the TPA final state S_n, respectively; and $\Delta\mu_k$ is the dipole moment difference between S_0 and S_k, which is neglected in symmetric molecules. So for symmetric molecules, eq 5 becomes the following:[11,24]

$$\delta \propto \frac{M_{0k}{}^2 M_{kn}{}^2}{(E_{0k} - E_{0n}/2)^2\Gamma} \quad (6)$$

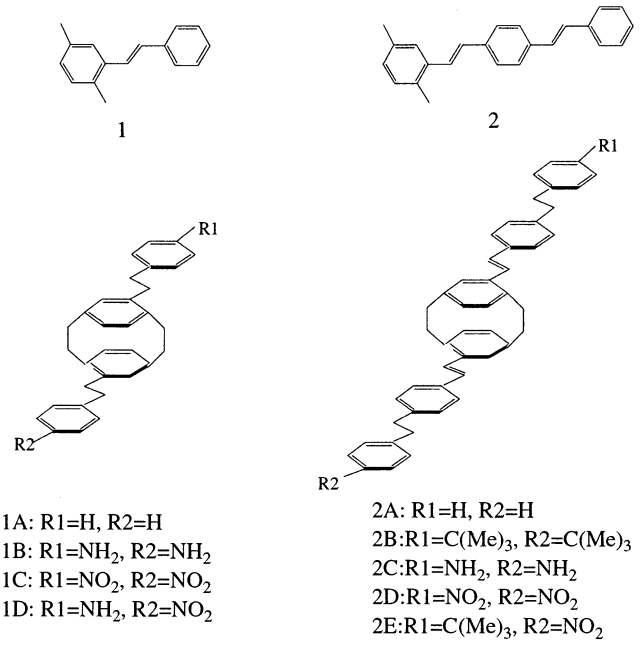

1A: R1=H, R2=H
1B: R1=NH_2, R2=NH_2
1C: R1=NO_2, R2=NO_2
1D: R1=NH_2, R2=NO_2

2A: R1=H, R2=H
2B:R1=$C(Me)_3$, R2=$C(Me)_3$
2C:R1=NH_2, R2=NH_2
2D:R1=NO_2, R2=NO_2
2E:R1=$C(Me)_3$, R2=NO_2

Figure 1. Molecular structure designs for the studied compounds.

In principle, any kind of self-consistent-field molecular orbital (SCFMO) procedure combined with the configuration interaction (CI) can be used to calculate the physical values in the above expression. In this paper, considering the size of the studied molecules, the semiempirical AM1 was primarily used to calculate the molecular equilibrium geometry. Then, the property of electronic excited states was obtained by 169 singly (SCI) and 11 doubly (DCI) excited configurations using the ZINDO program. Furthermore, either the UV−vis (ground-state one-photon absorption) spectra or the transition dipole moment and the corresponding transition energy that were needed to predict TPA were provided. Then, according to eqs 1−4, the second hyperpolarizability γ and TPA cross section $\delta(\omega)$ were calculated.

3. Results and Discussions

3.1. Structural Design and Geometry Optimization. The molecular structures were chosen according to Figure 1. All molecular equilibrium geometries are attained by the semiempirical AM1 method. The third-order nonlinear optical effect of organic conjugated systems arises from the delocalization of their π electrons. On the basis of the compounds reported in the literature,[28] we designed a series of paracyclophane derivatives. First, we designed two parent monomeric chromophores—stilbene derivative 1 and distyrylbenzene derivative 2. Then, on the basis of 1 and 2, we built two primary backbones—1A and 2A—which correspond to dimers of 1 and 2. Subsequently, we introduce different donors ($C(Me)_3$, NH_2) and a different acceptor (NO_2) to change the donor or acceptor strength and the arrangement of molecules; consequently, 1B, 1C, 1D, 2B, 2C, 2E, and 2D are formed. As shown in Figure 1, although the molecule is drawn flat here for clarity, ring strain distorts the phenyl rings in the paracyclophane core. In the literature,[21] authors showed that the distance between bridgehead carbons

TABLE 1: Maximum One-Photon Absorption and Transition Nature for Compounds

molecule	transition	$\lambda^{(1)}$/nm	f
1	$S_0 \rightarrow S_1$	294.6 (293)[27]	0.49859
1A	$S_0 \rightarrow S_3$	364.4	0.32820
	$S_0 \rightarrow S_5$	316.9 (315)[27]	0.73593
1B	$S_0 \rightarrow S_3$	364.1	0.44532
	$S_0 \rightarrow S_5$	320.4	1.22510
1C	$S_0 \rightarrow S_3$	382.1	0.52675
	$S_0 \rightarrow S_7$	331.2	0.73033
1D	$S_0 \rightarrow S_3$	374.1	0.42910
	$S_0 \rightarrow S_6$	324.6	0.83594
2	$S_0 \rightarrow S_1$	321.9	1.78039
2A	$S_0 \rightarrow S_3$	367.5	1.48937
	$S_0 \rightarrow S_5$	331.3	2.06660
2B	$S_0 \rightarrow S_3$	365.5 (372)[27]	1.86214
	$S_0 \rightarrow S_5$	332.0	1.90031
2C	$S_0 \rightarrow S_3$	366.5	2.19736
	$S_0 \rightarrow S_5$	334.7	1.75304
2D	$S_0 \rightarrow S_3$	367.8	2.36033
	$S_0 \rightarrow S_5$	330.2	1.43474
2E	$S_0 \rightarrow S_3$	368.9	1.75562
	$S_0 \rightarrow S_5$	333.4	1.87200
M	$S_0 \rightarrow S_1$	325.2 (322)[29]	1.38310

TABLE 2: Two-Photon Absorption Properties of Molecules

molecule	transition	$\lambda^{(2)}$ (nm)	$\gamma \times 10^{-34}$/esu	δ_{max} (cm^4 s/photon)
1	$S_0 \rightarrow S_4$	471.4	$-0.7305 + 3.937i$	**365.867**
1A	$S_0 \rightarrow S_7$	572.0	$-2.927 + 11.12i$	702.232
	$S_0 \rightarrow S_{15}$	492.0	$-12.39 + 18.61i$	**1587.71**
1B	$S_0 \rightarrow S_{10}$	568.0	$-4.142 + 29.05i$	**1859.31**
	$S_0 \rightarrow S_{15}$	495.6	$-22.52 + 10.57i$	889.009
1C	$S_0 \rightarrow S_{11}$	598.6	$-18.03 + 24.98i$	1439.85
	$S_0 \rightarrow S_{18}$	504.8	$-24.53 + 21.12i$	**1711.78**
1D	$S_0 \rightarrow S_8$	619.6	$0.7361 + 31.66i$	1703.14
	$S_0 \rightarrow S_{17}$	501.8	$-34.35 + 21.82i$	**1789.46**
2	$S_0 \rightarrow S_5$	537.6	$3.298 + 37.51i$	**2680.38**
2A	$S_0 \rightarrow S_{11}$	572.8	$-14.28 + 70.13i$	4414.58
	$S_0 \rightarrow S_{17}$	506.6	$-51.13 + 107.9i$	**8679.39**
2B	$S_0 \rightarrow S_{13}$	572.8	$-13.28 + 80.01i$	5036.01
	$S_0 \rightarrow S_{19}$	501.2	$-110.6 + 122.0i$	**10033.0**
2C	$S_0 \rightarrow S_{13}$	573.2	$-12.21 + 87.86i$	5522.33
	$S_0 \rightarrow S_{19}$	504.0	$-113.7 + 155.4i$	**12638.6**
2D	$S_0 \rightarrow S_{11}$	577.6	$-20.52 + 78.96i$	4887.72
	$S_0 \rightarrow S_{18}$	501.8	$-117.1 + 120.2i$	**9854.69**
2E	$S_0 \rightarrow S_{11}$	576.2	$-22.22 + 85.94i$	5345.79
	$S_0 \rightarrow S_{19}$	498.6	$-113.5 + 96.25i$	**7996.83**
M	$S_0 \rightarrow S_4$	517.4(529)[11]	$-0.5124 + 34.99i$	**429.712 (411)**[29]

on opposing rings is about 2.78 Å, which is larger than our result by 0.1 Å, whereas the distance between rings measured from the nonbridging carbon−carbon bonds is approximately 3.09 Å compared with the average value of 3.04 Å that we have obtained. It is obvious that our calculations are in agreement with the values in the literature.

3.2. One-Photon Absorption. Table 1 lists the calculated and experimental (given in parentheses) wavelength $\lambda_{max}^{(1)}$, which is with oscillator strength larger than 0.3, as well as the oscillator strength f and the nature of the transition for the maximum one-photon absorption (OPA) of every molecule. To examining the calculation method, we choose 4,4′-bis(dimethylamino) stilbene (molecule M in Table 1) as a comparison sample. As shown in Table 1, the results we calculated are in agreement with experimental values. As displayed in Table 1 and Figure 2a, comparing with one absorption peak of molecule 1, there appear to be two absorption peaks with longer wavelength and larger oscillator strengths in molecules 1A to 1D. This change is caused by the paracyclophane bridge functioning as a multidimensional tunneling barrier to increase the scope of the π-electron delocalization. A red shift of 22.3 nm is observed in the maximum absorption peak of the 3D dimer 1A relative to that of the 1-D parent molecule 1, and the oscillator strength is doubled. On the basis of 1A, different combinations of donor (NH_2) and acceptor (NO_2) groups have slightly dissimilar effects on the OPA spectra. The D/D pair substituent 1B has the strongest impact on the oscillator strength, resulting in a 66% increase, whereas the A/A substituent 1C provides the largest wavelength shifting of up to 14.3 nm. However, the overall effects of amino and nitro groups on the OPA spectra are not very large.

The most important parameter for determining the OPA intensities of active TPA materials seems to be the molecular length. Attaching 4-styryl-stilbene to 1, thereby creating 2, has several consequences for the OPA spectra. The $\lambda_{max}^{(1)}$ value exhibits a bathochromic shift by 27.3 nm, and the oscillator strength is increased by a factor of 2.6. From Figure 2b, comparing 2S (S = A−E) with 1S (S = A−D), we can find the same trend as that of 2 relative to 1. That is, the $\lambda_{max}^{(1)}$ value increases significantly and the oscillator strength changes by a factor of 2 or 3. It is notable that there are always two peaks, centered at 365 and 330 nm, with the same excited states in the OPA spectra of 2A to 2E. In this type of molecule, the introduction of donors ($C(Me)_3$, NH_2) and an acceptor (NO_2) still has a negligible impact on the OPA spectra.

As far as this series of paracyclophane derivatives is concerned, the most interesting finding from the simulations of the OPA spectra of the molecules considered here is that the molecular length and the dimensionality of the molecules are the most significant parameters in determining the OPA intensity. The choice of the donor and acceptor has a small impact on the OPA.

3.3. Two-Photon Absorption. Table 2 summarizes the position of the maximum TPA ($\lambda_{max}^{(2)}$) and the nature of the transition. According to expressions 1−4, we compiled a program to calculate the third-order optical susceptibility γ and the TPA cross section $\delta(\omega)$. Using the program, we calculated the real and imaginary parts of γ as well as the δ_{max} values, which are also listed in Table 2. As shown in Table 2, the results we calculated are in agreement with experimental values. In this paper, we have employed two methods to ensure the position of the TPA maximum $\lambda_{max}^{(2)}$. One is that according to eq 5—the three-state approximation—we select the excited states with the largest M_{0k} and M_{kn} values (shown in Table 3) and regard the n state as the final state of TPA, equal to the position of the maximum TPA ($\lambda_{max}^{(2)}$). Another way is to depict the TPA spectra for all of the compounds by considering the 25 lowest excited states point by point and consequently obtain the maximum TPA cross section δ_{max} in the TPA spectrum and the corresponding final state of TPA $\lambda_{max}^{(2)}$. But this method contains two conditions. First, for the molecules that have central symmetry such as 1A, 1B, 2C, and 2D, two-photon transitions must have initial and final states with the same parity. The transitions starting from the ground state (typically an even-symmetry state A_g) are concerned; therefore, the TPA allows only the even-parity excited states A_g to be identified. Consequently, we should select the excited states with A_g symmetry in the 25 lowest excited states and take them as the possible TPA final states to perform the calculations of the TPA cross sections. Second, for the molecule without a center of inversion symmetry such as 1, 2, 1D, and 2E, every state is of mixed parity, and hence between all electronic states, involving any number of photons is allowed. So for the 25 lowest excited states, every state has the possibility of being the TPA final state.

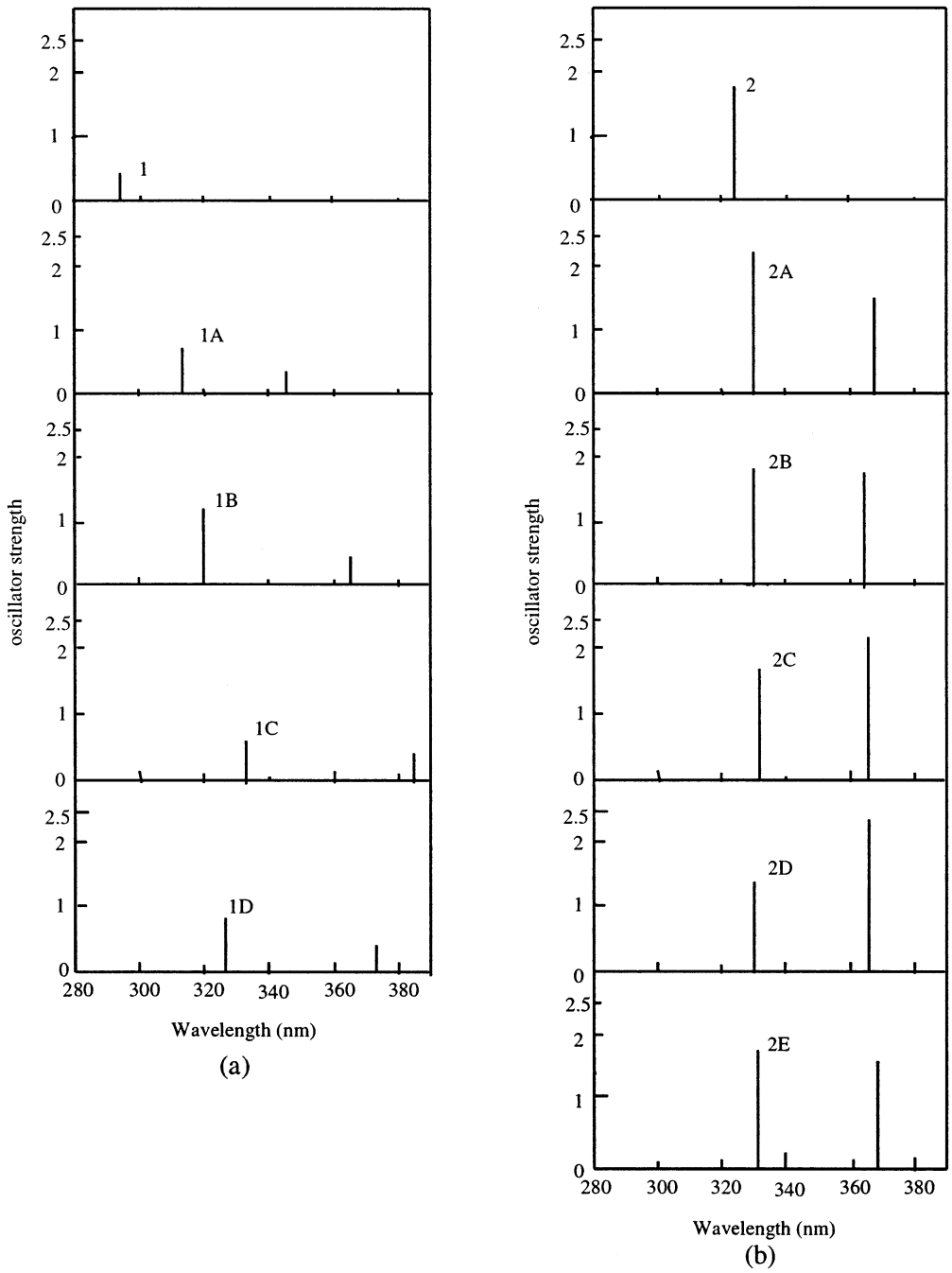

Figure 2. Absorption peaks *f* for the low-lying singlet states of molecules.

TABLE 3: Electronic Transition and Transition Dipole Moment of Compounds for Maximum TPA

molecule	$S_0 \rightarrow S_n$	M_{0k} (debye)	$M_{kn} + \Delta\mu_k$ (debye)	E_{ok} (eV)	E_{on} (eV)	Γ (eV)	$\{M_{0k}^2(M_{kn} + \Delta\mu_k)^2]/[(E_{0k} - E_{0n}/2)^2\Gamma]$	δ_{max} (10^{-50}cm^4 s/photon)
1	$S_0 \rightarrow S_4$	5.59	7.13	4.21	5.26	0.08	7954.2	365.867
1A	$S_0 \rightarrow S_{15}$	7.14	7.93	3.91	5.04	0.11	14664.6	1587.71
1B	$S_0 \rightarrow S_{10}$	5.87	9.12	3.40	5.00	0.10	35381.9	1859.31
1C	$S_0 \rightarrow S_{18}$	7.17	9.95	3.74	4.91	0.11	28021.1	1711.78
1D	$S_0 \rightarrow S_{17}$	7.59	12.49	3.82	4.94	0.11	52287.2	1789.46
2	$S_0 \rightarrow S_5$	11.02	10.30	3.85	4.61	0.08	77112.8	2680.38
2A	$S_0 \rightarrow S_{17}$	12.06	8.57	3.74	4.89	0.11	57461.5	8679.39
2B	$S_0 \rightarrow S_{19}$	11.57	12.68	3.73	4.95	0.11	103492.1	10033.0
2C	$S_0 \rightarrow S_{19}$	11.16	13.97	3.70	4.92	0.11	143709.4	12638.6
2D	$S_0 \rightarrow S_{18}$	10.03	11.38	3.75	4.94	0.11	72289.2	9854.69
2E	$S_0 \rightarrow S_{19}$	11.51	16.17	3.72	4.97	0.11	206463.9	7996.83

As shown in Table 2 and Figure 3, in which the segments of the TPA cross sections larger than zero are shown and the dominating TPA states of all of the studied molecules are illustrated, except 1 and 2, there are two TPA peaks in the compounds, centered at 570 and 500 nm. The impact of the introduction of the donor and acceptor, the increased conjugated

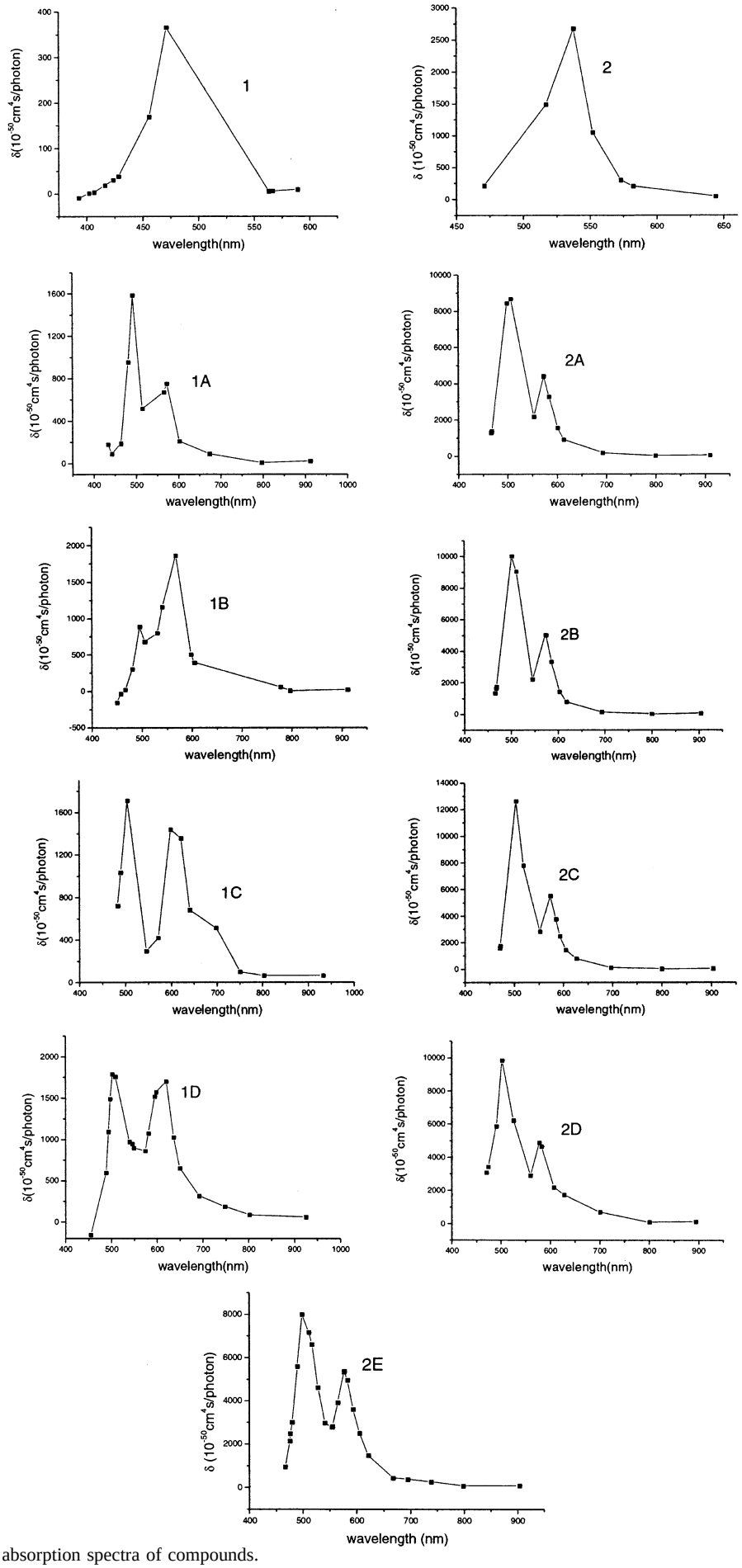

Figure 3. Two-photon absorption spectra of compounds.

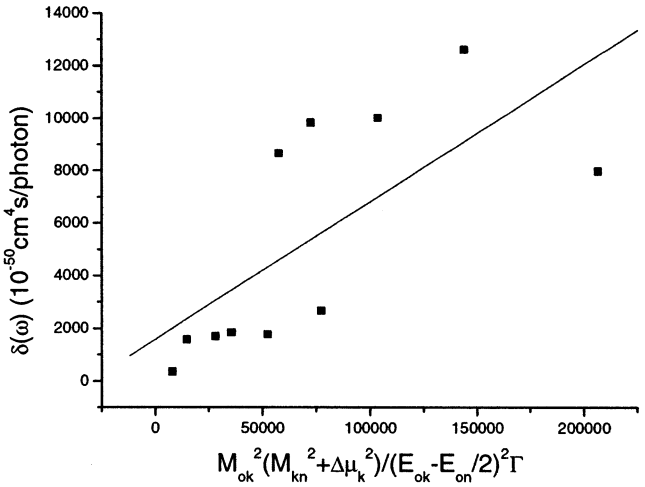

Figure 4. Plot of δ_{max} vs $M_{0k}^2(M_{kn} + \Delta\mu_k)^2/(E_{0k} - E_{0n}/2)^2\Gamma$.

length, and the enhanced dimensionality on the position of maximum TPA wavelength $\lambda_{max}^{(2)}$ is small. However, these effects on the TPA cross sections are quite substantial. This can be seen from the results of 1-based compounds listed in Table 2. The 3-D dimer 1A has increased the TPA cross section of 1-D parent monometic dye 1 by more than 4 times, from 365.867×10^{-50} cm^4 s/photon to 1589.71×10^{-50} cm^4 s/photon. On the basis of 1A, different donor/acceptor substituents have slightly improved the TPA cross section by about $(150-300) \times 10^{-50}$ cm^4 s/photon.

Comparing 2S (S = A−E) with 1S (S = A−D), we find that the conjugated length plays a crucial role in the performance of TPA materials. The TPA cross section of 2 is found to be around 2680.38×10^{-50}cm^4 s/photon, which is larger than that of 1 (365.867×10^{-50}cm^4 s/photon) by more than 7 times. The maximum TPA cross section of 2A is about 6 times that of its counterpart 1A. As shown in Table 2 and Figure 3, the TPA cross section of 2C (12638.6×10^{-50}cm^4 s/photon) is 120% that of 2B (10033.0×10^{-50}cm^4 s/photon) simply because of the change in the donor group from $C(Me)_3$ to NH_2. Therefore, the use of a stronger donor has very positive effects on the TPA cross sections. An important role is played by the molecular symmetry. The two D/D paired molecules 2B and 2C have the largest TPA cross sections. The maximum TPA cross sections of symmetrical D/D and A/A structures are higher than those for the asymmetrical D/A arrangements by $(2000-4000) \times 10^{-50}$ cm^4 s/photon. Our calculated results have thus confirmed the experimental findings on the importance of molecular symmetry.[11]

According to the results in Tables 2 and 3, the relationship between the maximum TPA cross section δ_{max} of every compound and $M_{0k}^2(M_{kn} + \Delta\mu_k)^2/(E_{0k} - E_{0n}/2)^2\Gamma$ is depicted in Figure 4. As can be seen, the calculated points are averagely distributed on the two sides of the line. The results in Figure 4 confirm that the position and relative strength of the two-photon resonance for these derived paracyclophanes are to be predicted using expression 5. It is obvious that the changing trend of TPA cross sections predicted by two different methods above are in accord with each other.

From Table 2, one can find that for every molecule every TPA peak has its own origin. We take 2E as the example to analyze their sources. As shown in Figure 5, the first OPA peak of 2E comes from the mixing of electron transitions from HOMO to LUMO, HOMO to LUMO + 1, HOMO to LUMO + 2, and HOMO to LUMO + 6. The transitions from HOMO to LUMO, HOMO to LUMO + 2, and HOMO to LUMO + 6 are equal to the charge transition from the central paracyclophane bridge to the acceptor part, and these transitions are connected to the molecular in-plane *y* axis and the out-of-plane *z* axis. The transition from HOMO to LUMO + 1 mainly concentrates on the central part to the donor moiety. In other words, the first OPA peak of 2E mainly comes from the charge transfer from the center part to the two sides. The second OPA peak of 2E is rooted in the mixing of electron transitions from HOMO − 2 to LUMO, HOMO − 1 to LUMO + 1, and HOMO − 1 to LUMO + 2, which are also displayed in Figure 5. The electron transfer from HOMO − 2 to LUMO mainly focuses on the interior of the acceptor segment, and the transition from HOMO − 1 to LUMO + 1 mostly focuses on the inside of the donor part. The charge transfer from the donor moiety to the acceptor side is equal to the transition from HOMO − 1 to LUMO + 2. From the above results, one can find that the second OPA peak of 2E comes from the charge transfer in the interior of the acceptor, the interior of the donor, and from the donor part to the acceptor branch. These results are consistent with the investigations in ref 30.

Figure 6 depicts the electron transitions corresponding to the two TPA peaks of 2E. In comparison to that of OPA in Figure 5, it can be seen that the two OPA peaks of 2E come from the mixing of some electron transitions, whereas the configurations of the electron transitions of the two TPA peaks are single. As shown in Figure 6, the first TPA peak is mainly made up of the electron transition from HOMO to LUMO, which also contributes to the first OPA peak. It is obvious that for a asymmetric molecule such as 2E every state is of mixed parity and the one-photon allowed excited state can also equally be the two-photon allowed excited state. For the second TPA peak of 2E, it comes from the electron transition from HOMO − 3 to LUMO + 1, which is equal to the charge transfer from the center part to the donor moiety. In balance, the electron transitions relative to the TPA peaks of 2E are equal to the charge transfer from the center part to the two sides.

Theoretically and experimentally, both methods—attaching strong electron-donating and electron-withdrawing groups to the π-conjugated molecules and the extension of the π-conjugated length—are proven to enhance the NLO properties of organic molecules, which are quite often hampered by an optical transparency problem. It causes the bathochromic shift of the $\pi-\pi^*$ absorption band, and thus the requirement of high transparency to visible light will not be met. The calculation shows that the maximum TPA cross section of 2S (S = A−E) is 6 times as that of its counterpart 1S (S = A−D) whereas $\lambda_{max}^{(1)}$ has no obvious red shift. Gompper et al. [31] pointed out that the maximum wavelength $\lambda_{max}^{(1)}$ of the electronic spectra of the chromophore molecules of the nonlinear optical materials ought to be shorter than 415 nm so that the transparency can be guaranteed. From the calculated electronic spectra listed in Table 1, it can be seen that $\lambda_{max}^{(1)}$ of all of the molecules is lower than 385 nm (i.e., the third-order susceptibility and the TPA cross section increase without lowering the transparency). The TPA materials with high transparency can be applied to the synthesis of optical limiting device.[32,33] Examining the absolute values of the real parts of the second hyperpolarizabilties, one can find that the magnitude of this parameter for all molecules ranges from 10^{-34} to 10^{-32} esu. Thus, it can be concluded that this type of paracyclophane derivative will be a kind of third-order nonlinear optical and TPA material from the viewpoint of the high transparency and the relatively large NLO response.

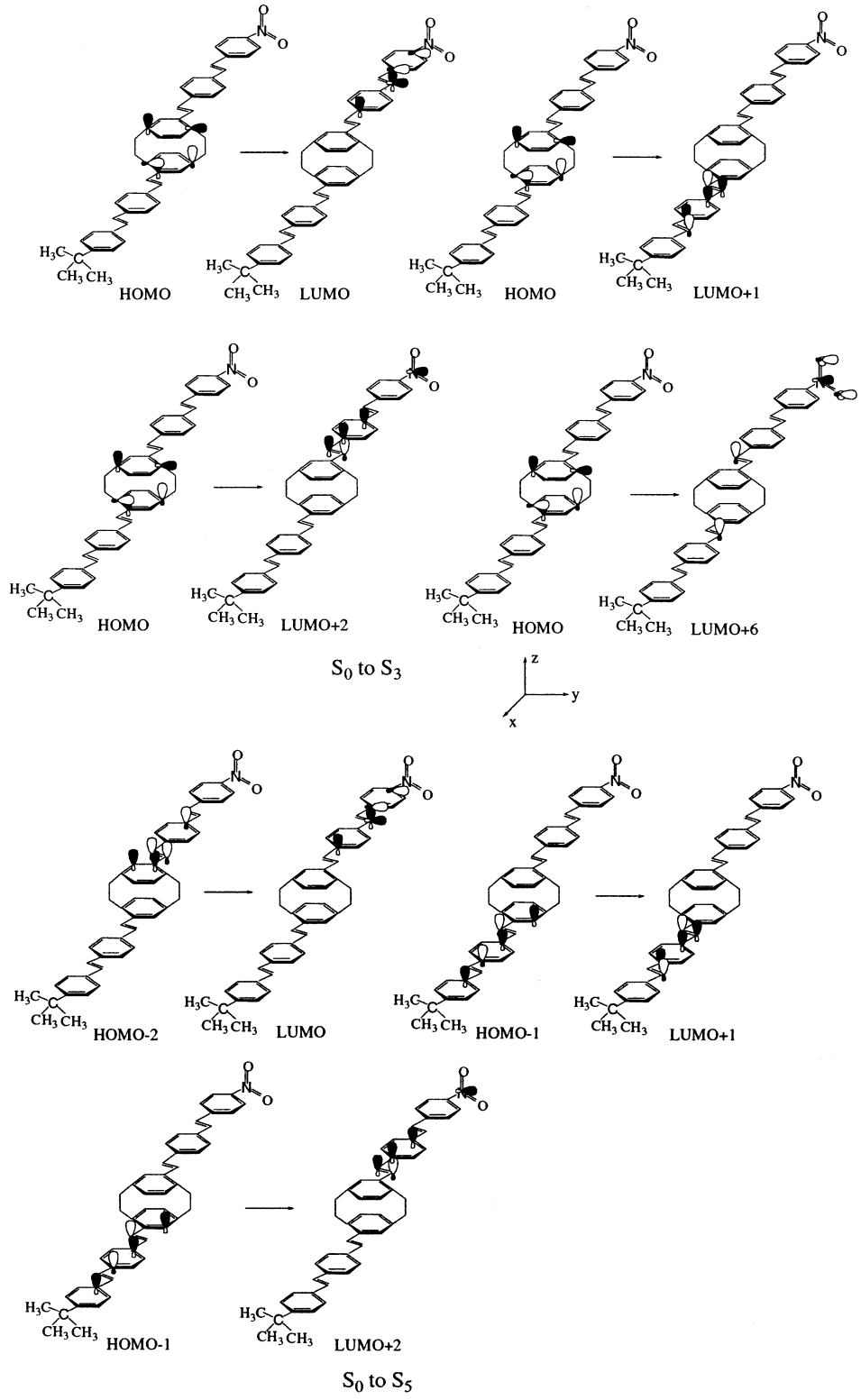

Figure 5. Atomic orbital composition of the HOMO − 2, HOMO − 1, HOMO, LUMO, LUMO + 1, LUMO + 2 and, LUMO + 6 of 2C

Most conventional molecular designs for the various NLO applications are based on intramolecular charge-transfer (ICT) processes from a donor to an acceptor moiety through a π-electron conjugated path such as stilbene, azobene, or thiophene derivatives. Recently, more and more attention has been paid to novel molecular engineering schemes. Among them, "through-space" electronic interactions between donor and acceptor groups are interesting and promising. The experimental observations and the theoretical calculations[34] have proven that the paracyclophane molecular template can be used as the cornerstone of a new strategy for through-space charge transfer (TSCT) mediated and controlled by $\pi-\pi$ stacking within the cyclophane moiety. In this paper, we will discuss the properties of TSCT in paracyclophane derivatives by means of analyzing the Muliken charge distributions in molecules. We take the molecule 2E as the example to carry out the analysis. Figure 7 shows the Muliken charge distribution of the molecule 2E in the ground state and in the fifth excited state. As displayed in Figure 7, either in the ground state or in the excited state the electron in the molecule is indeed transferred from the donor

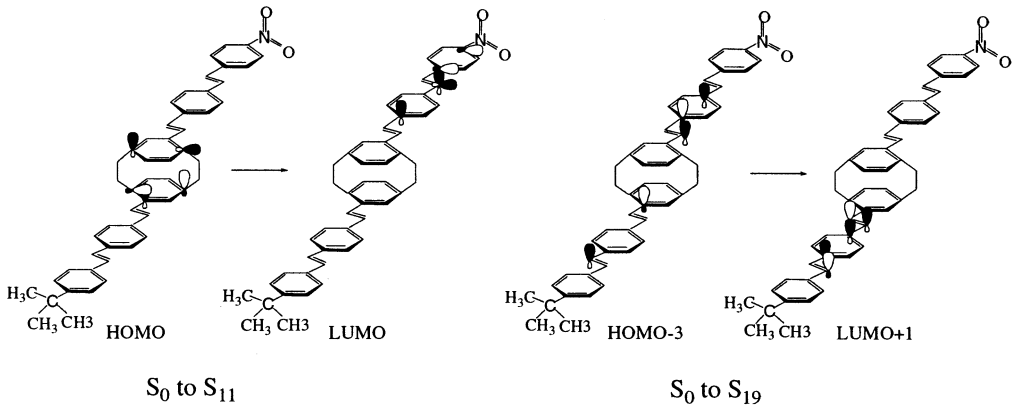

Figure 6. HOMO − 3, HOMO, LUMO, and LUMO + 1 atomic orbitals of 2C.

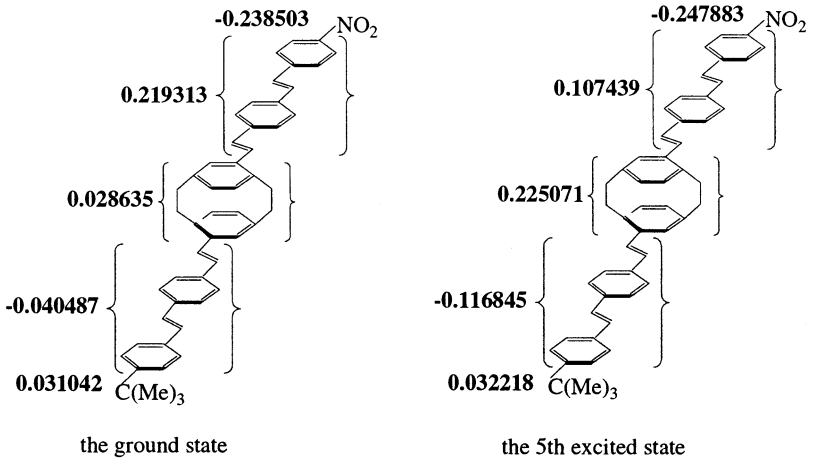

Figure 7. Muliken charge distributions of compound 2C.

$C(Me)_3$ to the acceptor NO_2 as it is in the conventional molecules. But the fact that the electron does not transfer unblockedly is reflected by the negative charge centered at the moiety between the donor and the paracyclophane part. This results from the "obstacle" role of the paracyclophane in the form of a $\pi-\pi$ stack, which is in good agreement with the conclusion in ref 34. From above the result, we find that as for the paracyclophane derivatives the paracyclophane as an obstacle blocks the charge transfer but does not stop this process by TSCT. It is important that they possess high transparency and significantly enhance the TPA cross section. As a consequence, the paracyclophane derivatives are promising NLOs, in particular, TPA materials.

4. Conclusions

In this paper, the one- and two-photon absorption properties of a series of paracyclophane derivatives have been investigated. The results show that not only on the OPA spectra but also on the TPA spectra the conjugated length of the molecules has the most important effect. The 3-D dimers formed by the connection of the paracyclophane bridge have TPA cross sections that are 4 times larger than those of the 1-D parent monometic molecules. Our calculated results have confirmed the experimental finding of the importance of molecular symmetry. Paracyclophane-based molecules can be classified as a completely new and promising kind of nonlinear optical material from the standpoint of the high transparency and relatively large NLO response. The paracyclophane molecular template as a novel strategy for through-space charge transfer is worth investigating further.

Acknowledgment. This work was supported by the National Nature Science Foundation of China (20273023, 90101026) and the Key Laboratory for Supramolecular Structure and Material of Jilin University.

References and Notes

(1) Bhawalkar, J. D.; He, G. S.; Prasad, P. N. *Rep. Prog. Phys.* **1996**, *59*, 1041.
(2) He, G. S.; Zhao, C.-F.; Bhawalkar, J. D.; Prasad, P. N. *Appl. Phys. Lett.* **1995**, *67*, 3703.
(3) Zhao, C.-F.; He, G. S.; Bhawalkar, J. D.; Park, C. K.; Prasad, P. N. *Chem. Mater.* **1995**, *7*, 1979.
(4) Fleitz, P. A.; Sutherland, R. A.; Stroghendl, F. P.; Larson, F. P.; Dalton, L. R. *SPIE Proc.* **1998**, *3472*, 91.
(5) He, G. S.; Bhawalkar, J. D.; Zhao, C.-F.; Prasad, P. N. *Appl. Phys. Lett.* **1995**, *67*, 2433.
(6) Ehrlich, J. E.; Wu, X.-L.; Lee, I.-Y. S.; Hu, Z.-Y.; Röeckel, H.; Marder, S. R.; Perry, J. W. *Opt. Lett.* **1997**, *22*, 1843.
(7) Bhawalkar, J. D.; Kumar, N. D.; Zhao, C.-F.; Prasad, P. N. *J. Clin. Laser Med. Surg.* **1997**, *15*, 201.
(8) Denk, M.; Strickler, J. H.; Webb, W. W. *Science (Washington, D.C.)* **1990**, *248*, 73.
(9) Xu, C. M. J.; Webb, W. W. *Opt. Lett.* **1995**, *20*, 2532.
(10) Wu, E. S.; Stricker, J. H.; Harrell, W. R.; Webb, W. W. *SPIE Proc.* **1992**, *1674*, 776.
(11) Albota, M.; Beljonne, D.; Brédas, J. L.; Ehrlich, J. E.; Fu, J.; Heikal, A. A.; Hess, S. E.; Kogej, T.; Levin, M. D.; Marder, S. R.; McCord-Maughon, D.; Perry, J. W.; Röeckel, H.; Rumi, M.; Subramaniam, G.; Webb, W. W.; Wu, X.; Xu, C. *Science (Washington, D.C.)* **1998**, *281*, 1653.
(12) Reinhardt, B. A.; Brott, L. L.; Clarson, S. J.; Dillard, A. G.; Bhatt, J. C. Kannan, R.; Yuan, L.; He, G. S.; Prasad, P. N. *Chem. Mater.* **1998**, *10*, 1863.
(13) Chung, S.-J.; Kim, K.-S.; Lin, T.-C.; He, G. S.; Swiatkiewicz, J.; Prasad, P. N. *J. Phys. Chem. B* **1999**, *103*, 10741.
(14) Kim, O.-K.; Lee, K.-S.; Woo, H. Y.; Kim, K.-S.; He, G.S.; Swiatkiewicz, J.; Prasad, P. N. *Chem. Mater.* **2000**, *12*, 284.
(15) Norman, P.; Luo, Y.; Ågren, H. *J. Chem. Phys.* **1999**, *111*, 7758.

(16) Kogej, T.; Beljonne, D.; Meyers, F.; Perry, J. W.; Marder, S. R.; Brédas, J. L. *Chem. Phys. Lett.* **1998**, *298*, 1.

(17) Lee, W.-H.; Lee, H.; Kim, J.-A.; Choi, J.-H.; Cho, M.; Jeon, S.-J.; Cho, B. R. *J. Am. Chem. Soc.* **2001**, *123*, 10658.

(18) Fuks-Janczarek, I.; Nunzi, J. M.; Sahraoui, B.; Kityk, I. V.; Berdowski, J.; Caminade, A. M.; Majoral, J. P.; Martineau, A. C.; Frere, P.; Roncali, J. *Opt. Commun.* **2002**, *209*, 461.

(19) Zhou, X.; Ren, A.-M. Feng, J.-K.; Liu, X.-J. *Chem. Phys. Lett.* **2002**, *362*, 541.

(20) Zhou, X.; Ren, A.-M.; Feng, J.-K.; Liu, X.-J.; Zhang, J.-X. Liu, J.-Z. *Phys. Chem. Chem. Phys.* **2002**, *4*, 4346.

(21) Voegtle, F. *Cyclophane Chemistry;* Wiley & Sons: New York, 1993.

(22) Tsuge, A.; Nishimoto, T.; Uchida, T.; Yasutake, M.; Moriguchi, T.; Sakata, K. *J. Org. Chem.* **1999**, *64*, 7246.

(23) Caylor, C. L.; Dobrianow, I.; Kimmr, C.; Thome, R. E.; Zipfel, W.; Webb, W. W. *Phys. Rev. E* **1999**, *59*, R3831.

(24) Dick, B.; Hochstrasser, R. M.; Trommsdorff, H. P. In *Nonlinear Optical Properties of Organic Molecules and Crystals;* Chemla, D. S., Zyss, J., Eds.; Academic Press: Orlando, FL, 1987; Vol. 2, pp 167−170.

(25) Orr, B. J.; Ward, J. F. *Mol. Phys.* **1971**, *20*, 513.

(26) Beljonne, D.; Cornil, J.; Shuai, Z.; Bredas, J. L.; Rohlfing, F.; Bradlley, D. D. C.; Torruellas, W. E.; Ricci, V.; Stegeman, G. I. *Phys. Rev. B* **1997**, *55*, 1505.

(27) Garito, A. F.; Heflin, J.R.; Wong, K.Y.; Zamani-Khamiri, O. In *Organic Materials for Nonlinear Optics;* Hann, R.A., Bloor, D., Eds.; Royal Society of Chemistry: London, 1989; p 16.

(28) Bartholomew, G. P.; Bazan, G. C. *Acc. Chem. Res.* **2001**, *34*, 30.

(29) Morel, Y.; Irimia, A.; Najechalski, P.; Kervella, Y.; Stephan, O.; Baldeck, P. L.; Andraud, C. *J. Chem. Phys.* **2001**, *114*, 5391.

(30) Moran, A. M.; Bartholomew, G. P.; Bazan, G. C.; Kelly, A. M. *J. Phys. Chem.* **2002**, *106*, 4928.

(31) Gompper, R.; Mair, H. J.; Polborn, K. *Synthesis* **1997**, *6*, 696.

(32) Stiel, H.; Volkmer, A.; Rückmann, I.; Zeug, A.; Ehrenberg, B.; Röder, B. *Opt. Commun.* **1998**, *155*, 135.

(33) Zhang, C.; Song, Y.; Kühn, F. E.; Wang, Y.; Xin, X.; Herrmann, W. A. *Adv. Mater.* **2002**, *14*, 818.

(34) Zyss, J.; Ledoux, I.; Volkov, S.; Chernyak, V.; Mukamel, S.; Bartholomew, G. P.; Bazan, G. C. *J. Am. Chem. Soc.* **2000**, *122*, 11956.